American Journal of Traffic and Transportation Engineering
2023; 8(6): 128-134
http://www.sciencepublishinggroup.com/j/ajtte
doi: 10.11648/j.ajtte.20230806.11
ISSN: 2578-8582 (Print); ISSN: 2578-8604 (Online)

Exploring the Application of Computational Fluid Dynamics (CFD) Wind Environment Simulation in the Layout of Port Operation Areas

Lixiong Chen*, Dongkui Wu, Chun Shen

Merchant Marine College, Shanghai Maritime University, Shanghai, China

Email address:
chenlixiong2002@163.com (Lixiong Chen), wudk@shmtu.edu.cn (Dongkui Wu), chunshen@shmtu.edu.cn (Chun Shen)

*Corresponding author

To cite this article:
Lixiong Chen, Dongkui Wu, Chun Shen. Exploring the Application of Computational Fluid Dynamics (CFD) Wind Environment Simulation in the Layout of Port Operation Areas. *American Journal of Traffic and Transportation Engineering*. Vol. 8, No. 6, 2023, pp. 128-134.
doi: 10.11648/j.ajtte.20230806.11

Received: October 4, 2023; **Accepted**: November 2, 2023; **Published**: November 11, 2023

Abstract: The wind environment in port areas not only affects port planning and layout but also constrains the navigation time window during operations. During the engineering certification process for port construction, typically only monthly and yearly climatic characteristics of hydrological and meteorological conditions, as well as statistical conclusions on the main weather systems causing high winds and waves in the region, can be considered. These data alone cannot represent the wind and wave distribution in specific operational areas. Sometimes, it is necessary to refer to the wind and wave characteristics of the operational waters for specific port operation point selection. In such cases, remote sensing or simulation techniques, such as computational fluid dynamics (CFD), are used to infer the wind and wave distribution characteristics. Taking Shanghai Yangshan Deepwater Port as an example, the design of the pilot boarding point for strong winds and waves is located near the main channel, providing limited protection against high winds and waves. On average, there are 11.9 instances of pilot traffic control caused by high winds and waves each year. To mitigate the impact of severe weather on port operations, it is proposed to move the temporary boarding point for pilots in strong winds and waves westward to the east gate closer to the port area. Traditional hydrological and meteorological statistical data cannot support the selection of the new area, so it was decided to use CFD technology to simulate the wind environment in the relevant island and reef area and analyze the wind field distribution under different wind directions. Combined with the three-year statistical data from the meteorological station on Xiaoyangshan Island, a new area for the temporary pilot boarding point was selected. The CFD wind environment simulation results provided the primary technical support for determining the reference area.

Keywords: Pilot Boarding Points, Island and Reef Areas, Computational Fluid Dynamics, Wind Environment Simulation

1. Introduction

The efficient and safe operation of ports is the foundation of global trade and commerce [1]. The layout and design of port operational areas directly impact operational efficiency and safety [2, 3]. Traditional methods of port operational area layout mainly rely on experience and are difficult to accurately assess the impact of meteorological factors on port operations. Especially in island and reef areas around ports, due to complex terrain, water currents, and wind conditions, safe navigation of ships faces higher requirements [4]. The setting of pilot boarding points can effectively support the work of pilots, ensuring their safe boarding and accurate guidance of ships through island and reef areas. Therefore, the reasonable layout of pilot boarding points is also an important part of the layout and design of port operational areas [5]. This involves selecting appropriate locations, providing good visibility and passage conditions, and considering the safety of pilots boarding/disembarkation.

To assess the impact of hydro-meteorological elements on port operations [6], traditional port construction certification processes usually summarize the monthly and annual statistical climate characteristics of strong winds and create wind frequency charts as estimates for port operating time. However,

for specific port operational site selection and other issues, it is necessary to refer to the wind and wave distribution characteristics of the operating waters, which cannot be met by traditional statistical data. Therefore, it becomes necessary to use techniques such as remote sensing or simulation to infer wind and wave distribution characteristics [7]. In this regard, Computational Fluid Dynamics (CFD) is a powerful simulation tool. It can simulate fluid flow [8], heat transfer, and other physical phenomena [9] in a virtual environment, providing valuable insights for complex systems and promoting design and process optimization. In the layout of port operational areas, CFD wind environment simulation technology can simulate and visualize the airflow dynamics within the port area and its surroundings [10]. By simulating wind environments under different operating conditions, the risk status of port operational areas can be evaluated, and the layout of operational areas can be optimized. This will help port managers better plan and manage port operations, improve operational efficiency and safety, and provide scientific decision support.

Therefore, the scientific and precise layout and design of port operational areas are crucial for the efficient and safe operation of ports. By accurately assessing the impact of meteorological factors and utilizing techniques such as CFD to optimize the layout, port operational efficiency and safety can be enhanced, providing stable and reliable port services for global trade and commerce.

2. The Importance of Setting Reasonable Pilot Boarding Points (Using Yangshan Deepwater Port as an Example)

Setting reasonable pilot boarding points is crucial for ship safety and navigation efficiency. Firstly, selecting suitable pilot boarding points can ensure that pilots board the ship at the optimal location, improving boarding efficiency and ensuring that pilots can arrive at the ship promptly to begin navigation work. Secondly, reasonable pilot boarding points can improve ship safety by ensuring that pilots can board the ship safely and smoothly, providing timely guidance and reducing the probability of accidents. In addition, setting reasonable pilot boarding points can also improve navigation efficiency by reducing the distance between the ship and the shore, shortening pilot boarding time, and improving work efficiency. In summary, setting reasonable pilot boarding points is essential for ship safety and navigation efficiency [11]. Therefore, port management departments should set pilot boarding points based on specific conditions.

Yangshan Deepwater Port is located at the intersection of the Yangtze River estuary and Hangzhou Bay, north of the Yangtze River estuary, east of Huangze Yang, and south of the Zhoushan Islands (as shown in Figure 1). The port area and nearby waters are often affected by adverse weather conditions. The pilot boarding point for large wind waves in Yangshan Deepwater Port is designed near the main channel. However, due to the general shielding conditions of the entrance channel, there are an average of 11.9 traffic controls caused by large wind waves each year. Under large wind wave conditions, suspension of pilotage operations causes large container ships to be unable to enter or leave the port normally, seriously affecting port production efficiency.

To expand the operating time window of Yangshan Deepwater Port, reduce the impact of large wind wave weather on port production, ensure ship navigation safety, and improve the success rate of pilotage during large wind waves, on the premise of ensuring safety, pilots will be sent to board the ship at a temporary boarding point closer to the east gate and with better boarding conditions. As shown in Figure 2, the original large wind wave pilotage operation area on the main channel of Yangshan Port will be moved westward to a suitable area between Huxiao Island and Shaoji Island. To determine the specific area, CFD simulation technology will be used for intuitive display.

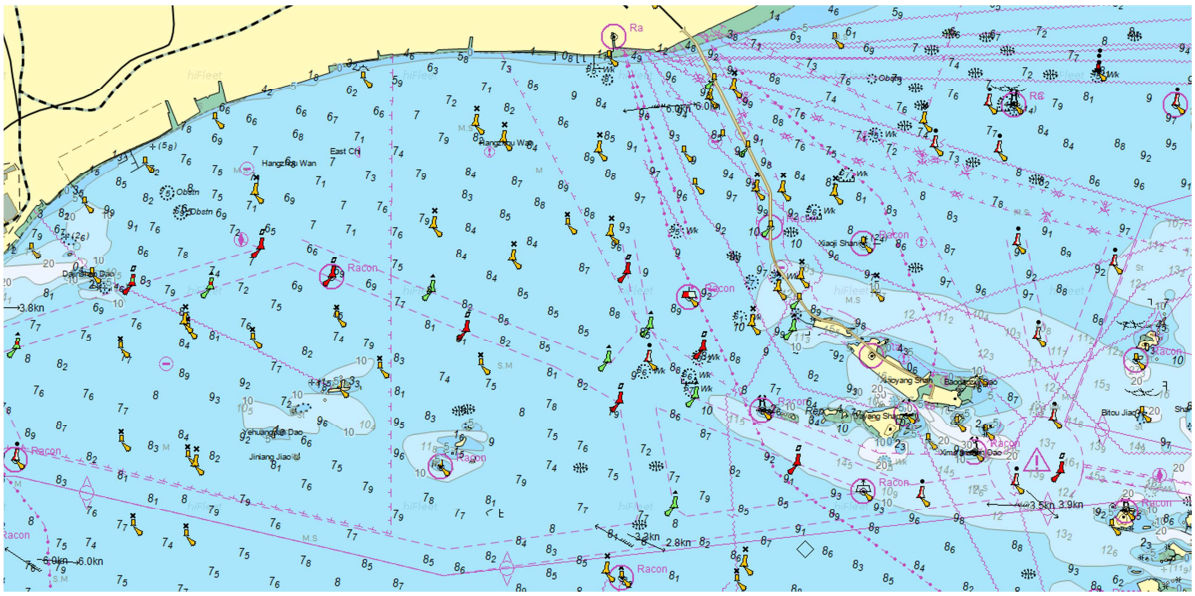

Figure 1. *Nautical Chart of Yangshan Deepwater Port and its Adjacent Waters.*

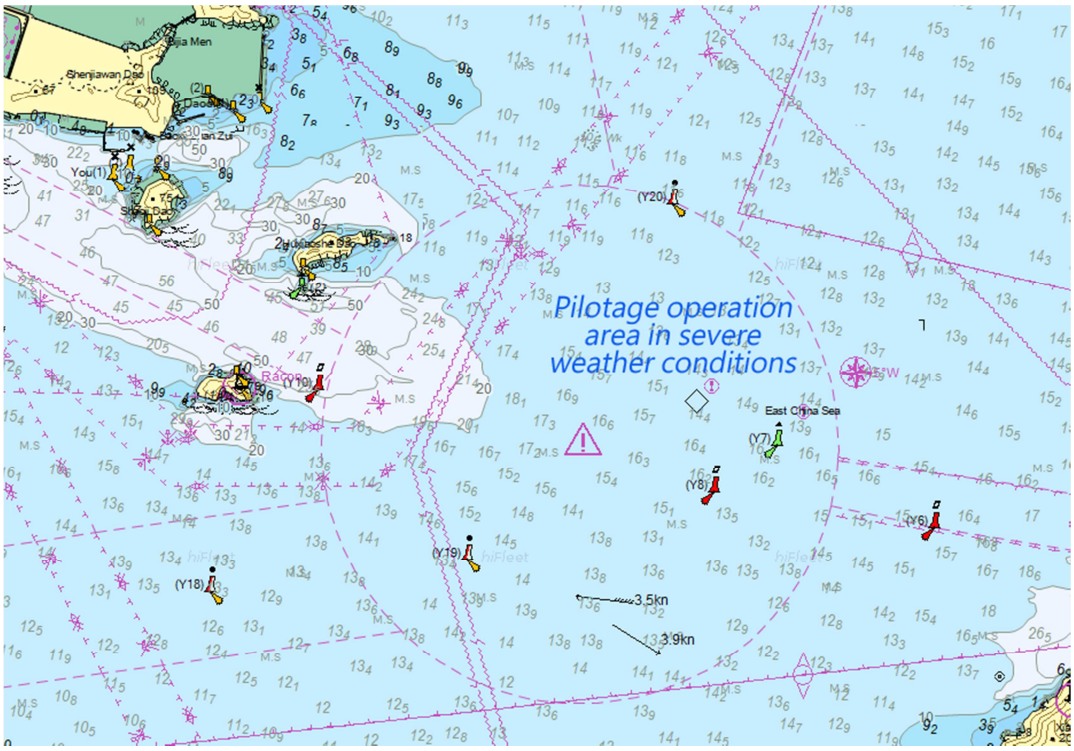

Figure 2. *Traditional pilot embarkation area for strong winds and waves at Yangshan Port and the selected relocation area to the west.*

3. Application of Computational Fluid Dynamics in Determining Pilot Boarding Points in Yangshan Deepwater Port

3.1. Selection of Research Objects

Using the electronic chart software of the Merchant Marine College of Shanghai Maritime University, the land of Yangshan Port was exported as two-dimensional DWF format data. To reduce the calculation amount, the entire land was reduced by a scale of 1000 times, and the three pieces of land surrounded by Shaoji Island, Huxiaoshe Island, and Xima'an Island were selected in AutoCAD (as shown in Figure 3). At the same time, small areas around the islands were removed, and the distribution of wind in the water surrounded by the three islands was analyzed.

Wind fields have strong randomness and uncertainty. When conducting CFD calculations, a large-scale benchmark calculation domain needs to be selected for preliminary calculations. According to the research results of the local standard "Technical Regulations for Numerical Simulation of Building Environment" in Shanghai, if the maximum characteristic scale of the research object is L, the length and width of the calculation domain in the horizontal direction should be extended by 4-6L respectively, and the height in the vertical direction should be 3-6L. When the focus of the simulation is the wake field behind the building, the length of the downwind direction should be expanded to 6L or more [12].

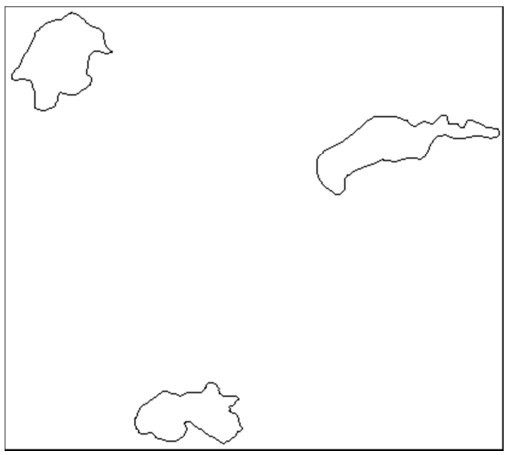

Figure 3. *Two-dimensional models of Shaoji Island, Huxiaoshe Island, and Xima'an Island.*

In order to simulate the distribution of wind direction and wind around the four base points and four corner points in eight directions in the water surrounding the small islands, we decided to use the maximum characteristic scale of Huxiaoshe Island as L, and simulate the areas of approximately 5L and 10L respectively at the entrance, top, left and right sides (taking the west wind entrance as an example, as shown in Figure 4). The model data was imported into ICEM, and the three small islands were separated from other calculation areas in the surface operation, and then the small island parts were removed. One of the eight directions was selected as the entrance, its opposite side was set as the exit, and both sides and the small island were selected as wall surfaces. Finally, grid division was performed, and some grid results are shown in Figure 5.

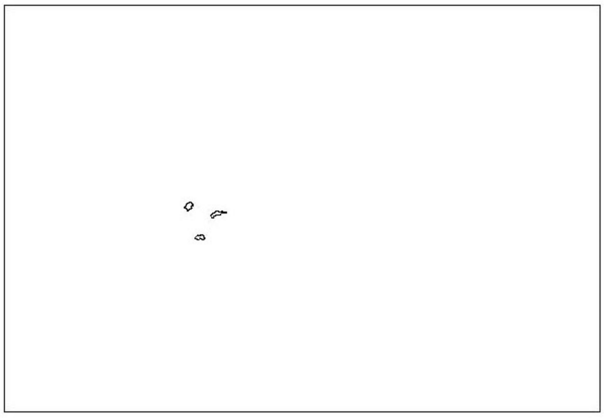

Figure 4. *Computational domain selected for simulation.*

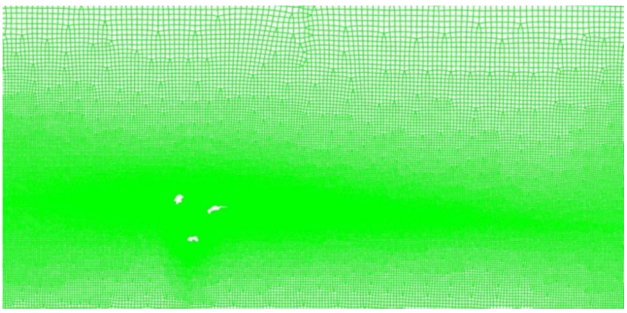

Figure 5. *Partial meshing result of the computational domain imported into ICEM.*

3.2. Boundary Conditions Setting

The Reynolds number Re of the flow around the cylinder can be calculated using formula 1, where the air density is taken as 1.293 kilograms per cubic meter, velocity is 18 meters per second, and the east-west length of Huxiaoshe Island in CAD is 1.4 meters. The dynamic viscosity of air is taken as 1.79×10^{-5} Pa·s. Based on the calculation, the Reynolds number is determined to be 5.8×10^{6}, indicating fully developed turbulence. Therefore, a turbulence model is selected, specifically the k-ε turbulence model.

$$Re=\rho vd/\mu \quad (1)$$

According to the "Announcement on the Publication of Supplementary or Revised Pilotage Waters of Major Ports in China" (Announcement No. 13 of 2021) issued by the Ministry of Transport, the deep-water channel of the Yangtze River estuary and the southern channel of the Yangtze River estuary have been designated as areas for pilotage operations in strong winds and waves. According to the regulations in the announcement, the weather restrictions for using the pilotage operation area in strong winds and waves are: forecasted wind force ≥ 8 and wave height ≥ 1.5 meters. According to the Beaufort wind scale, wind force 8 refers to wind speeds between 17.2-20.7 meters per second. Therefore, the entrance wind speed is set to 18 meters per second in the simulation.

After creating a grid model in ICEM, import it into Fluent. In the Fluent interface, you can check the following settings: display proportions, inlet, outlet, and wall settings. In the model options, select the k-ε turbulence model and set air as the fluid, leaving the solid option at its default setting. In the boundary conditions, set the direction of the inlet as a velocity inlet with a velocity size of 18 meters per second, and set the outlet as a pressure outlet as set in ICEM. In the solution algorithm interface, use the SIMPLE algorithm and select the default settings in the solution control scheme interface. After initialization, set the iteration number to 200, check the convergence curve for adjustments if necessary, and then start calculating the model. [12].

3.3. Simulation Wind Field Distribution

If the west wind of 18 meters per second is taken as the inlet, the corresponding east direction is the pressure outlet, and the south, north sides and three small islands are the wall surfaces, the wind distribution around the three small islands simulated can be seen in Figure 6. The following observations can be made from the figure: on the west side of Shaoji Island and Huxiaoshe Island, due to the island's eddy current effect, the wind near the edge of the island is stronger, even exceeding eight-level wind; the wind in the water far away from the island is similar to that at the inlet; and on the east side of the island, due to the island's shielding effect, the wind is weaker, far less than eight-level wind.

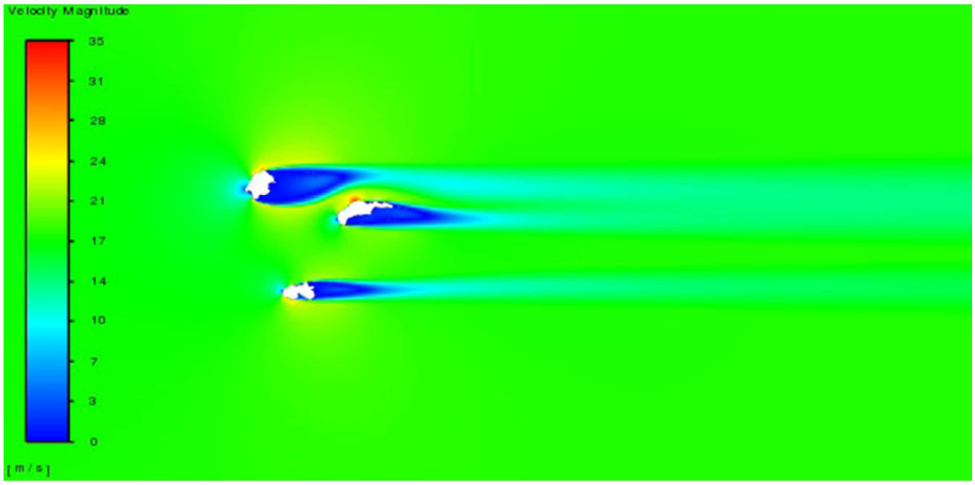

Figure 6. *Overview of wind speed distribution in the water area under Beaufort scale 8 west wind (18 m/s) around the three islands.*

3.4. Grid-Independence of Calculation Results

When conducting numerical simulations, it is necessary to construct dense grids around the target object, while sparse grids should be used in areas far from the target object to improve the accuracy of the calculation results and reduce the number of grids. If the transition from sparse to dense grids is too rapid, it may lead to a decrease in grid quality and affect the convergence of the calculation [13]. In studies on grid independence [14、15], the maximum grid size can be set in ICEM to control the number of grids. Different maximum grid sizes can be set, such as 10, 5, 2, 1, 0.5, 0.25, and 0.125, and then the generated grids can be imported into Fluent to calculate the wind velocity distribution in the computational domain. The wind velocity at the center point of the computational domain is taken as the validation point, and the obtained results are shown in Table 1. The correspondence between the wind velocity at the center point of the computational domain exported from Fluent and the number of grids is shown in Figure 7.

Table 1. *Correspondence between the number of grid cells formed by setting the maximum grid size in ICEM and the wind speed at the center point of the simulation domain.*

Maximum grid size	**10**	**5**	**2**	**1**	**0.5**	**0.25**	**0.125**
Number of grid cells	5739	6813	8922	15919	37299	80170	222926
Wind speed at the center point	divergence.	15	16.12	14.4	14.49	14.28	14.27

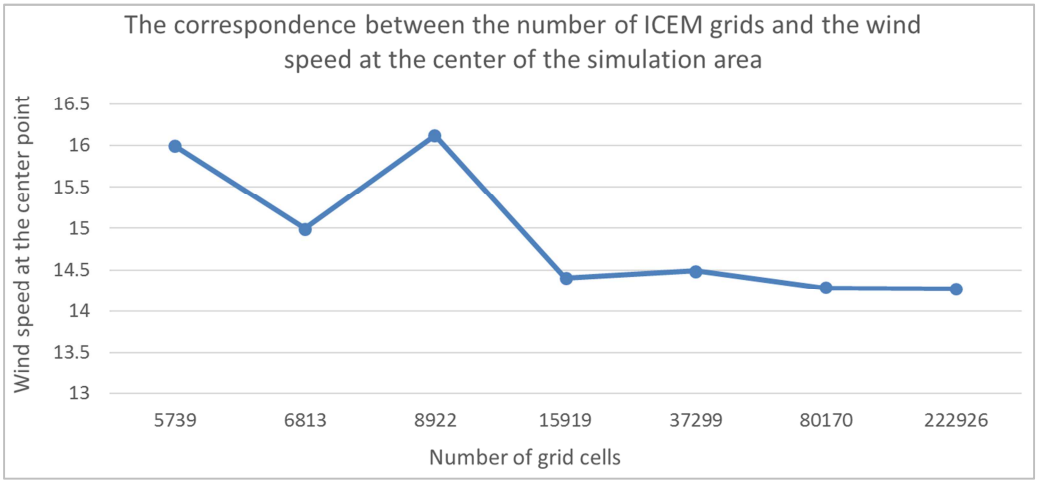

Figure 7. *Relationship between the wind speed at the center point of the computational domain exported from Fluent and the number of grid cells.*

From Table 1 or Figure 7, it can be observed that if the number of grids is too small in ICEM, it may lead to non-convergence in Fluent. As the number of grids increases, the wind velocity distribution in the study area can be simulated. As the number of grids continues to increase, the simulation results gradually stabilize. When the maximum grid size is set to 1 or smaller in ICEM, the simulation results no longer exhibit significant fluctuations with an increase in the number of grids, indicating a weak correlation with the grid quantity. The simulated wind velocity distribution remains essentially unchanged.

4. The Application of Wind Environment Simulation in the Determination of Pilot Boarding Points at Yangshan Port

4.1. Statistical Analysis of Strong Winds Based on Meteorological Data on Xiaoyangshan Island

Strong winds are one of the common severe weather conditions on islands, mainly caused by typhoons, cold air intrusion, and cyclones passing through. Due to the geographical environment and underlying surface characteristics of Yangshan Port, there are more days with strong winds in the port area. Based on the measured data from the Xiaoyangshan Meteorological Station (at a height of 49 meters) of Shanghai Marine Meteorological Observatory, the statistical information on wind speeds of force 7 and above at Yangshan Island in Yangshan Port from 2018 to 2020 has been compiled, as shown in Table 2.

The main channel of Yangshan Deepwater Port runs roughly northwest-southeast, and the influence of the island and reef topography causes a funneling effect to occur in the wind direction roughly aligned with the main channel, resulting in stronger winds in this direction than in others. Based on observation data from Xiaoyangshan Island from 2018 to 2020, statistical analysis was conducted on the wind direction of strong winds of force 7 and above. The results showed that the northwest to north winds occurred for 66 days in 2018, accounting for 54% of the total days; for 64 days in 2019, accounting for 58% of the total days; and for 73 days in 2020, accounting for 63% of the total days. In terms of monthly distribution, the number of days with strong winds of

force 7 and above was highest in December, with an average of 16 days, followed by August, November, and January. In contrast, the number of days with strong winds in June and July was relatively low.

Table 2. *Statistics of wind force at Beaufort scale 7 and above on Xiaoyangshan Island from 2018 to 2020.*

year	Days with Strong Wind	Average Wind Speed	Wind Direction	Percentage (%)
2018	122	17.5	N	26.8
			NNW	17
			NW	16
			SE	15
2019	109	17.8	N	41.8
			NNW	11.0
			SSE	10.9
			NW	9.1
2020	115	16.9	N	42.2
			SSE	18.1
			NNW	11.2
			NW	8.6

4.2. Statistical Data on Operation Control at Yangshan Port Due to Strong Wind Impact

Based on the statistical data of operational restrictions at Yangshan Port from 2010 to 2020 due to weather and sea conditions, the results of wind-related restrictions were selected for analysis, as shown in Table 3.

Table 3. *Number of Days with Operational Control at Yangshan Port for Wind Force 7 and Above (Unit: days).*

Year \ Month	1	2	3	4	5	6	7	8	9	10	11	12
2011	2	0	1	1	0	3	0	3	0	0	0	6
2012	0	1	0	5	0	0	0	11	1	1	9	7
2013	0	0	1	1	0	3	1	0	0	5	6	5
2014	0	1	0	0	0	0	3	2	3	1	1	6
2015	3	0	1	2	0	0	3	0	0	1	4	4
2016	3	0	3	2	1	0	0	0	0	1	3	1
2017	2	1	0	0	0	0	0	0	3	6	0	0
2018	5	0	1	1	0	0	2	6	0	2	0	3
2019	0	0	0	0	0	0	0	2	4	2	2	3
2020	4	4	0	1	0	0	0	3	2	0	0	3
Average	1.9	0.7	0.7	1.3	0.1	0.6	0.9	2.7	1.3	1.9	2.5	3.8

According to the statistical data of operational restrictions at Yangshan Port from 2010 to 2020 due to strong winds and waves, the total number of days affected by strong winds and waves throughout the year was 18.4 days. Among them, December had the highest number of days affected by strong winds caused by cold high-pressure systems, with 3.8 days; followed by November and January. August had the second-highest number of days affected by strong winds caused by typhoon activity, with 2.7 days; followed by September. October was a month when both typhoon and cold high-pressure activities occurred simultaneously.

4.3. Discussion of Simulation Results

In the simulation, we set the wind speed to eight levels (18 meters per second) as the inlet wind speed of Fluent, and took the southern waters of Huxiaoshe Island as the research object. The results of the cloud map show that Huxiaoshe Island has the most obvious blocking effect on north and northwest winds, so the wind speed on the leeward side of the southern waters is much lower than eight levels. Similarly, if we select the southern waters of Xiaoji Island as the research object, the effect of northwest to north winds is similar to that of the southern waters of Huxiaoshe Island, but due to the shorter east-west length of Xiaoji Island, its blocking effect on wind is relatively weak, so the range of lower wind speeds is not as extensive as that of Huxiaoshe Island. Under other wind conditions, the southern waters of Huxiaoshe Island will experience varying degrees of wind attenuation due to the island's flow and blocking effects. For example, under south to southwest winds, the wind speed in the southern waters of Huxiaoshe Island is significantly lower than that in surrounding waters.

4.4. Discussion on the New Location of Temporary Pilot Boarding Point During Strong Winds and Waves

According to simulation results, when the wind direction of a wind of seven or higher levels is from northwest to north, moving the pilot's current operating area to the south of Huxiaoshe Island can significantly reduce the operation time affected by strong wind. However, under other wind conditions, the impact range is different from that of the northward wind, but the effect on extending operation time is not as significant as that of the northwest to north wind direction. The wind distribution of Xiaoji Island is similar to

that of Huxiaoshe Island, but due to the smaller east-west length of the island, the effect of improving operational conditions is relatively weak. Based on simulation results of the sheltering effect on the leeward side of islands and reefs and statistical conclusions that northwest to north winds account for more than half of winds of seven or higher levels on Xiaoyangshan Island, we suggest that in the new location selection for temporary pilot boarding point during strong winds and waves at Yangshan Deepwater Port, it is advisable to consider selecting a location along the main channel of Yangshan Port towards the east gate and combining it with other conditions on the south side of Huxiaoshe Island.

5. Conclusion

Conducting wind field environmental simulations using CFD technology in island and reef areas can visually display the distribution of wind environments around the islands and reefs under specific wind directions and speeds. These simulation results can provide strong technical support for port construction layout, site selection for temporary pilot boarding points during strong winds and waves, and other related considerations. In order to meet the requirement of moving the temporary pilot boarding point for Yangshan Port's strong winds and waves towards the east and closer to the entrance gate, we established models for Xiaoji Island, Huxiaoshe Island, and Xima'an Island, and conducted wind environment simulations using ANSYS. The results show that relocating the temporary mooring and departure point for strong winds and waves to the south of Huxiaoshe Island can provide better sheltering conditions for pilot operations during severe weather conditions, thereby expanding the operational time window of Yangshan Deepwater Port and reducing the impact of strong winds and waves on port operations.

References

[1] Ismail Kurt, Murat Aymelek, Operational adaptation of ports with maritime autonomous surface ships, Transport Policy, Volume 145, 2024, Pages 1-10, ISSN 0967-070X, https://doi.org/10.1016/j.tranpol.2023.09.023.

[2] Miguel Hervás-Peralta, Sara Poveda-Reyes, Francisco Enrique Santarremigia, Gemma Dolores Molero, Designing the layout of terminals with dangerous goods for safer and more secure ports and hinterlands, Case Studies on Transport Policy, Volume 8, Issue 2, 2020, Pages 300-310, ISSN 2213-624X, https://doi.org/10.1016/j.cstp.2020.01.006.

[3] Bowei Xu, Hailing Wang, Junjun Li, Evaluation of operation cost and energy consumption of ports: comparative study on different container terminal layouts, Simulation Modelling Practice and Theory, Volume 127, 2023, 102792, ISSN 1569-190X, https://doi.org/10.1016/j.simpat.2023.102792.

[4] Masashi Watanabe, Hironobu Kan, Ken Toguchi, Yosuke Nakashima, Volker Roeber, Taro Arikawa, Effect of the structural complexity of a coral reef on wave propagation: A case study from Komaka Island, Japan, Ocean Engineering, Volume 287, Part 1, 2023, 115632, ISSN 0029-8018, https://doi.org/10.1016/j.oceaneng.2023.115632.

[5] Jiao Yan, Zhuang Yanfeng. Discussion on the establishment of the water area for pilots to board and disembark from Qingdao Port in strong winds and waves [J]. Navigation, 2023 (04): 30-34.

[6] Monique O. Franzen, Elisa H. L. Fernandes, Eduardo Siegle, Impacts of coastal structures on hydro-morphodynamic patterns and guidelines towards sustainable coastal development: A case studies review, Regional Studies in Marine Science, Volume 44, 2021, 101800, ISSN 2352-4855, https://doi.org/10.1016/j.rsma.2021.101800.

[7] Putri Amelia, Artya Lathifah, Dynamics Analysis of Container Needs and Availability in Surabaya Container Terminal with Agent-Based Modeling and Simulation, Procedia Computer Science, Volume 161, 2019, Pages 910-918, ISSN 1877-0509, https://doi.org/10.1016/j.procs.2019.11.199.

[8] Arif Hussain, Adil Loya, Zeeshan Riaz, Saeed Akram Malik, To study the effectiveness of stern appendages (Cruciform & X Shaped configurations) for maneuverability of autonomous underwater vessel using computational fluid dynamics, Ocean Engineering, Volume 272, 2023, 113858, ISSN 0029-8018, https://doi.org/10.1016/j.oceaneng.2023.113858.

[9] A. Ricci, W. D. Janssen, H. J. van Wijhe, B. Blocken, CFD simulation of wind forces on ships in ports: Case study for the Rotterdam Cruise Terminal, Journal of Wind Engineering and Industrial Aerodynamics, Volume 205, 2020, 104315, ISSN 0167-6105, https://doi.org/10.1016/j.jweia.2020.104315.

[10] Francisco Toja-Silva, Takaaki Kono, Carlos Peralta, Oscar Lopez-Garcia, Jia Chen, A review of computational fluid dynamics (CFD) simulations of the wind flow around buildings for urban wind energy exploitation, Journal of Wind Engineering and Industrial Aerodynamics, Volume 180, 2018, P ages 66-87, ISSN 0167-6105 https://doi.org/10.1016/j.jweia.2018.07.010.

[11] Radwanski K., Rutkowski G. An Analysis of the Risks during Personnel Transfers between Units Operating on the Water. Water 2022, 14, 3303, https://doi.org/10.3390/w14203303.

[12] Ji Liang and Ge Caoyan. Research on Standardization of CFD Simulation Technology in Shanghai Local Standard "Technical Regulations for Building Environmental Numerical Simulation". Green Building, 2015, 7(05), 33-35.

[13] Munir Suner, Munip Bas, A new approach to narrow waterways traffic routing with potential flow theory and CFD, Ocean Engineering, Volume 261, 2022, 111862, ISSN 0029-8018, https://doi.org/10.1016/j.oceaneng.2022.111862.

[14] Shenghui Liu, Yanping Huang, Junfeng Wang, Theoretical and numerical investigation on the fin effectiveness and the fin efficiency of printed circuit heat exchanger with straight channels, International Journal of Thermal Sciences, Volume 132, 2018, Pages 558-566, ISSN 1290-0729, https://doi.org/10.1016/j.ijthermalsci.2018.06.029.

[15] Gu Mingheng, Zou Tingting, Xiang Jieqiong. Research on mesh independence of turbine blade structure design and vibration characteristics [J]. Internal Combustion Engine & Parts, 2021, (11): 8-9.